CDDpress

www.nature.com/cdd

ARTICLE

Check for updates

YB-1 is a positive regulator of KLF5 transcription factor in basal-like breast cancer

Dewei Jiang[1,2,12], Ting Qiu[1,2,12], Junjiang Peng[1,12], Siyuan Li[1,12], Tala[3], Wenlong Ren[1,4], Chuanyu Yang[1], Yi Wen[1], Chuan-Huizi Chen[5], Jian Sun[1,2], Yingying Wu[6], Rong Liu[7], Jun Zhou[3], Kongming Wu[8], Wen Liu[9], Xiaoyun Mao[10]✉, Zhongmei Zhou[1]✉ and Ceshi Chen[1,2,11]✉

Y-box binding protein 1 (YB-1) is a well-known oncogene highly expressed in various cancers, including basal-like breast cancer (BLBC). Beyond its role as a transcription factor, YB-1 is newly defined as an epigenetic regulator involving RNA 5-methylcytosine. However, its specific targets and pro-cancer functions are poorly defined. Here, based on clinical database, we demonstrate a positive correlation between Kruppel-like factor 5 (KLF5) and YB-1 expression in breast cancer patients, but a negative correlation with that of Dachshund homolog 1 (DACH1). Mechanistically, YB-1 enhances KLF5 expression not only through transcriptional activation that can be inhibited by DACH1, but also by stabilizing *KLF5* mRNA in a RNA 5-methylcytosine modification-dependent manner. Additionally, ribosomal S6 kinase 2 (RSK2) mediated YB-1 phosphorylation at Ser102 promotes YB-1/KLF5 transcriptional complex formation, which co-regulates the expression of BLBC specific genes, *Keratin 16 (KRT16)* and *lymphocyte antigen 6 family member D (Ly6D)*, to promote cancer cell proliferation. The RSK inhibitor, LJH685, suppressed BLBC cell tumourigenesis in vivo by disturbing YB-1-KLF5 axis. Our data suggest that YB-1 positively regulates KLF5 at multiple levels to promote BLBC progression. The novel RSK2-YB-1-KLF5-KRT16/Ly6D axis provides candidate diagnostic markers and therapeutic targets for BLBC.

Cell Death & Differentiation (2022) 29:1283–1295; https://doi.org/10.1038/s41418-021-00920-x

INTRODUCTION

Basal-like breast cancer (BLBC) largely overlaps with estrogen receptor (ER), progesterone receptor (PR), and HER2 triple negative breast cancer subgroup that has the poorest prognosis [1, 2], and there are limited therapeutics currently under clinical investigation for BLBC [3]. Kruppel-like factor 5 (KLF5), a member of the Sp/KLF family of transcription factors, functions as an oncogene in various cancers, including breast cancer, and especially BLBCs [4]. We previously reported that KLF5 promotes breast cancer cell proliferation and migration by regulating the transcription of *Cyclin D1*, *p27*, *FGF-BP1*, *mPGES1*, and *TNFAIP2* [5–8]. High levels of KLF5 expression in breast cancer are associated with poor patient survival [9]. In breast cancer cells, we demonstrated that KLF5 is transcriptionally induced by progesterone through PR [10] and dexamethasone through glucocorticoid receptor [11]. Additionally, KLF5 transcription is maintained by super enhancers [12]. However, the reason as to why KLF5 is specifically highly expressed in BLBC cannot be explained by these mechanisms.

Y-box binding protein 1 (YB-1), binding to both DNA [13] and RNA [14], plays important roles in physiological and pathological processes [15, 16]. YB-1 null mice are embryonic lethal and the mouse embryonic fibroblasts showed retarded cell growth compared to their wild type (WT) counterparts [17]. When acting as a transcription factor in the nucleus, YB-1 functions by binding to the inverted CCAAT motifs in the promoters of target genes, such as *CyclinD1*, *CD44*, *CD49f*, and *Nanog* [18–21]. YB-1 mainly located in the cytoplasm as an RNA-binding protein (RBP), regulating mRNA/tRNA stability or protein translation, for example, HIF1α [16]. Phosphorylation at YB-1 Ser102 by AKT, ERK, or RSK has been reported in a context-dependent manner [22–24]. YB-1 is a negative prognostic factor and an indicator of aggressiveness of several cancers [25, 26] and highly expressed in BLBC [8]. Dachshund homolog 1 (DACH1) is a well-known tumour suppressor that inhibits the transcription of oncogenes [27–29], partially through interaction with transcription factors, such as NCoR, Smads, ER, c-Jun, and YB-1 [30–33]. Compared to normal breast, and low-grade, and luminal-type breast cancers,

[1]Key Laboratory of Animal Models and Human Disease Mechanisms of Chinese Academy of Sciences & Yunnan Province, Kunming Institute of Zoology, Chinese Academy of Sciences, Kunming, China. [2]Kunming College of Lifesciences, University of Chinese Academy Sciences, Kunming, China. [3]State Key Laboratory of Medicinal Chemical Biology, College of Life Sciences, Nankai University, Tianjin, China. [4]College of Life Sciences, China University of Science and Technology, Hefei, Anhui, China. [5]School of Chinese Materia Medica, Yunnan University of Chinese Medicine, Kunming, China. [6]The First Affiliated Hospital, Kunming Medical University, Kunming, China. [7]The First Affiliated Hospital, Peking University, Beijing, China. [8]Department of Oncology, Tongji Hospital of Tongji Medical College of Huazhong University of Science and Technology, Wuhan, China. [9]School of Pharmaceutical Science, Fujian Provincial Key Laboratory of Innovative Drug Target Research, Xiamen University, Xiamen, China. [10]Department of Breast Surgery, The First Affiliated Hospital of China Medical University, Shenyang, China. [11]KIZ-CUHK Joint Laboratory of Bioresources and Molecular Research in Common Diseases, Kunming Institute of Zoology, Chinese Academy of Sciences, Kunming, China. [12]These authors contributed equally: Dewei Jiang, Ting Qiu, Junjiang Peng, Siyuan Li. ✉email: xymao@cmu.edu.cn; zhouzm@mail.kiz.ac.cn; chenc@mail.kiz.ac.cn

Edited by R De Maria

Received: 6 June 2021 Revised: 30 November 2021 Accepted: 2 December 2021
Published online: 13 January 2022

the expression of DACH1 is downregulated in breast carcinoma, high-grade, and basal-like tumours, respectively [29]. Recently, DACH1 was shown to suppress YB-1 mediated the regulation of KLF4 [27], a family member of KLF5.

In this study, we identified YB-1-KLF5-KRT16/Ly6D as a novel oncogenic axis that mediates BLBC cell growth that is inactivated by DACH1 re-expression or RSK inhibition. Our results support the potential application of this axis in BLBC diagnosis, prognosis, and treatment.

RESULTS

Expression of KLF5 is positively correlated with that of YB-1, but negatively correlated with DACH1 in breast cancer

We first sought to investigate the relationship among YB-1, DACH1, and KLF5 in BLBCs. YB-1 and KLF5 proteins were co-expressed in the two immortalized breast epithelial cell lines (MCF10A and 184B5) and BLBC cell lines (SUM149PT, HCC1937, and HCC1806); Both KLF5 and YB-1 proteins, were expressed at low levels in Luminal and HER2-positive breast cancer cell lines (HCC1500, MCF7, T47D, SKBR3, and JIMT1) and two BLBC breast cancer cell lines (BT549 and MDA-MB-468); In contrast, the expression pattern of DACH1 was contrary to that of KLF5 and YB-1 (Fig. 1A and Supplementary Fig. S1A). Analysis of the cancer genome atlas (TCGA) database also showed *KLF5* expression positively correlated with *YB-1* expression ($R = 0.4092$), whereas their expressions were negatively correlated with *DACH1* expression ($R = -0.3503$ and $R = -0.6051$, respectively) (Fig. 1B and Supplementary Fig. S1B). Kaplan-Meier plotter curves showed that high expression of KLF5 and YB-1 was significantly correlated with worse clinical outcomes in breast cancer patients; consistently, high DACH1 expression was significantly correlated with better clinical outcomes (Supplementary Fig. S1C). We further found that the expression of *YB-1* and *KLF5* was specifically high in BLBC and increased with pathological grades, whereas that of *DACH1* was specifically high in luminal tumours and decreased with pathological grades (Fig. 1C, D). Consistent with the mRNA expression pattern, immunohistochemical (IHC) staining showed positive expression of YB-1 and KLF5 in 78.1% of these specimens (Fig.1E, F). These results suggest that clinically there is a positive correlation between *YB-1* and *KLF5* expression, but a negative correlation between *DACH1* and *KLF5* expression in breast cancer.

YB-1 and DACH1 orchestrate *KLF5* transcription in BLBC cells

Next, we investigated whether YB-1 and DACH1 regulate KLF5 expression. We observed that the protein levels (Fig. 2A) and mRNA expression (Fig. 2B) of KLF5 and its downstream targets, CyclinD1 and FGF-BP1, were markedly reduced following YB-1 knockdown in both cell lines. A putative YB-1 binding site (−391 to −384 from the KLF5 start codon ATG) was identified in the *KLF5* proximal promoter (Fig. 2C). Next, we performed chromatin immunoprecipitation (ChIP) assays to find that YB-1 antibody, but not the control IgG, specifically pulled down the predicted *KLF5* promoter fragment (Fig. 2D). Luciferase reporter assay showed that the WT *KLF5* promoter, but not the YB-1 binding site mutant promoter, was significantly activated by YB-1 overexpression (Fig. 2E). We further performed oligo pull-down assays in vitro to demonstrate that only the WT biotinylated oligonucleotides, but not the mutant (MT) ones, efficiently pulled down YB-1 protein from cell lysates (Fig. 2F). These results suggest that YB-1 promotes *KLF5* transcription by directly binding to the CCAAT box in the *KLF5* promoter.

We further tested whether DACH1 inhibits YB-1-induced KLF5 expression. Overexpression of DACH1 completely blocked YB-1-induced KLF5 and Cyclin D1 expression in two cell lines (Fig. 2G and Supplementary Fig. S2A). Knockdown of DACH1 in HCC1806 increased YB-1 and KLF5 expression, which was blocked by simultaneous knockdown of YB-1 (Supplementary Fig. S2B). Interestingly, DACH1 bound to the *KLF5* promoter in a YB-1 dependent manner because knockdown of YB-1 significantly reduced the binding of DACH1 to the *KLF5* promoter (Fig. 2H). Consistently, DACH1 strongly inhibited YB-1-mediated *KLF5* promoter activation in HEK293T cells (Fig. 2I). We also demonstrated that DACH1 inhibited expression of *KLF5* and its downstream target genes *CyclinD1* and *FGF-BP1* depending on the DS domain of DACH1 (Fig. 2J, K and Supplementary Fig. S2C, D). Taken together, our data show that YB-1 is a positive transcriptional regulator of KLF5, while DACH1 suppresses YB-1-dependent KLF5 transcription.

YB-1 binds to and stabilizes m5C-modified *KLF5* mRNA in BLBC cells

YB-1 is recognized as an oncogenic RBP in various cancers [14, 16, 34]. Thus, we investigated whether YB-1 binds to *KLF5* mRNA. Native RNA binding protein immunoprecipitation (RIP) assay showed that YB-1 antibody strongly pulled down *KLF5* mRNA in both HCC1806 and HCC1937 cells (Fig. 3A, B). Recently, YB-1 was identified as a reader of RNA-m5C [35–37] that is catalysed by the NOP2/Sun RNA methyltransferase 2 (NSUN2) [38]. Coincidentally, NSUN2 is also highly expressed in BLBC and predicts worse outcomes in patients with breast cancer (Supplementary Fig. S3A, B). *KLF5* RNA sequences from six species contained four conserved YB-1-binding motifs [39] in coding regions (Supplementary Fig. S3C). We designed and synthesized five biotin-labelled *KLF5* mRNA truncates in vitro (Fig. 3C; Supplementary Fig. S3D) and incubated them with HCC1806 cell lysate. We observed that both YB-1 and NSUN2 were robustly pulled down mainly by B and C RNA fragments (Fig. 3D), both of which harbour the first/second predicted YB-1-binding sites. We knocked down endogenous YB-1 or NSUN2 and found that degradation of *KLF5* mRNA was accelerated (Fig. 3E), and YB-1 overexpression extended the half-life of *KLF5* mRNA (Supplementary Fig. S3E).

Data from RNA-m5C sequencing [35] showed a potential YB-1-binding site (star-marked) in *KLF5* mRNA in bladder cancer cells (Fig. 3C). Therefore, we mutated this site and the first/second sites separately (C to A) and found that any one of the mutations decreased the stability of fused transcripts (Fig. 3F). We then demonstrated that 5mC-RIP enriched *KLF5* transcripts (Fig. 3G), suggesting that *KLF5* mRNA was modified by m5C. Furthermore, we showed that YB-1 W65A (RNA-m5C binding disabled mutant) failed to rescue the KLF5 reduction induced by YB-1 depletion (Fig. 3H). Similarly, NSUN2 C321A (methyltransferase activity dead mutant) could not rescue the KLF5 reduction induced by NSUN2 depletion (Fig. 3I and Supplementary Fig. S3F). Consistently, the half-life of *KLF5* mRNA in HCC1937 cells was also extended by NSUN2 WT but not C321A mutant (Supplementary Fig. S3G). Taken together, these results suggest that NSUN2-mediated RNA-m5C modification and subsequent YB-1 binding stabilize *KLF5* mRNA in BLBC cells.

YB-1 promotes BLBC cell proliferation and tumour growth partially through KLF5

We wonder whether YB-1 promotes BLBC cell proliferation through KLF5. As expected, YB-1 depletion significantly reduced cell growth and DNA synthesis (Fig. 4A, B); DACH1 overexpression also inhibited cell growth and DNA synthesis in HCC1806 and HCC1937 cells, depending on the DS domain (Supplementary Fig. S4B–D). Furthermore, DACH1, but not its DS-deficient mutant, induced apoptosis, as indicated by the cleavage of caspase-3, PARP1, and annexin V staining (Supplementary Fig. S4E, F). Thus, we demonstrated that YB-1 promotes BLBC cell proliferation, while DACH1 inhibits cell proliferation and induces apoptosis. In addition, KLF5 overexpression significantly rescued the decrease in FGF-BP1 protein expression, cell viability, and DNA synthesis,

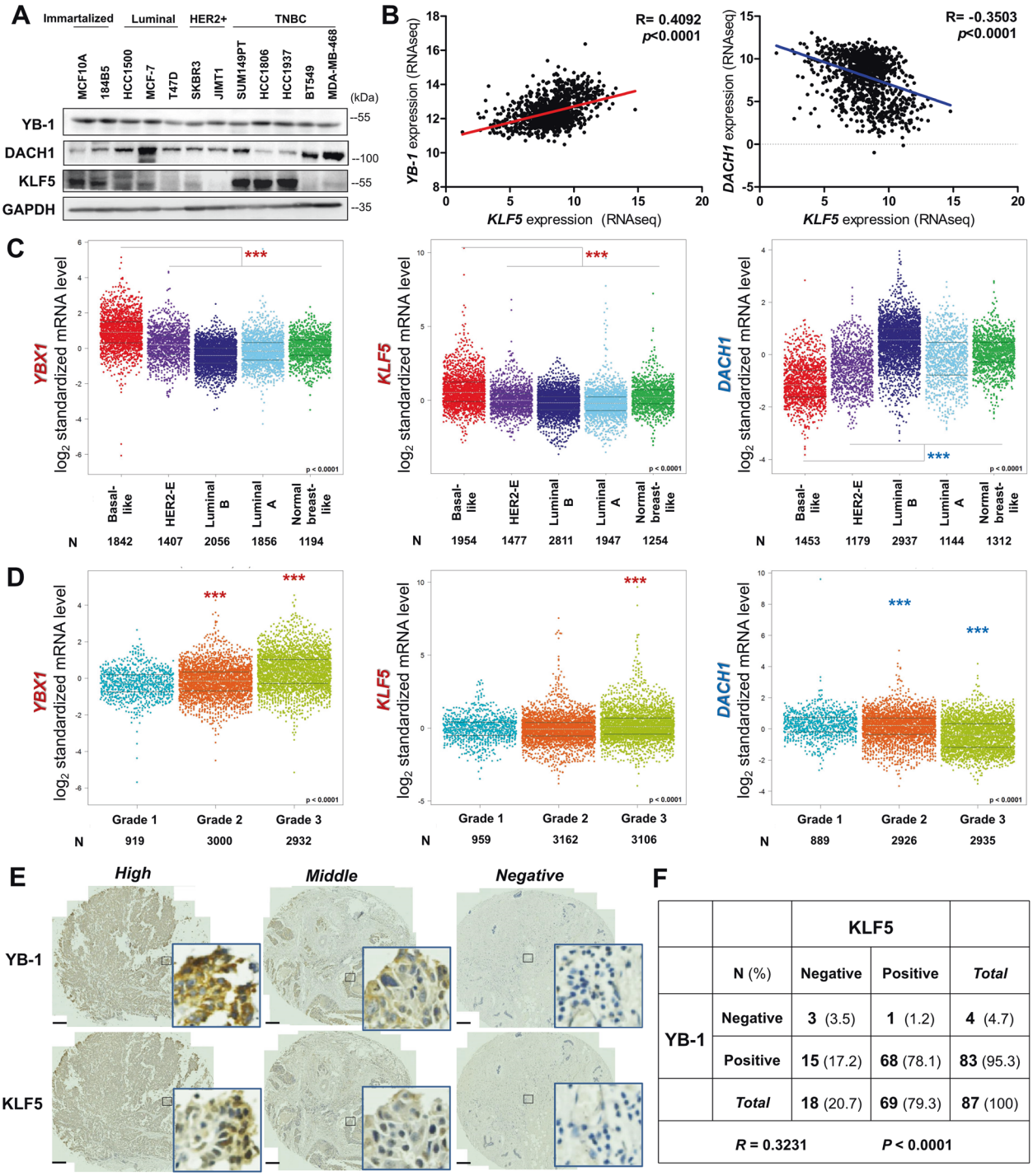

Fig. 1 KLF5 expression is positively correlated with YB-1 and negatively correlated with DACH1 in breast cancer. A Western blotting showed the expression of KLF5, YB-1 and DACH1 in immortalized mammary epithelial and breast cancer cell lines. **B** The analysis of expressional correlation among *KLF5*, *YB-1* (*YBX1*) and *DACH1* in breast cancer patients from the TCGA database. **C** The expression of *KLF5*, *YB-1* (*YBX1*) and *DACH1* of breast cancer patients classified with different PM50 subtypes and **D** pathological grades (bc-GenExMiner v4.5); ***$P < 0.0001$. **E** Representative images of IHC staining of YB-1 and KLF5 in BLBC specimens ($n = 87$, scale bar = 150 μm). **F** Pearson's correlation test of scored IHC staining in (**E**).

caused by YB-1-depletion (Fig. 4C–H). Consisitenty, the YB-1-depleted cancer cells grew significantly slower compared to the control cells (Fig. 4F) and the tumour weights of YB-1 knockdown xenografts were significantly lower than those of control xenografts (Fig. 4H). When KLF5 was overexpressed in the YB-1 knockdown cells, the YB-1 depletion-induced tumour growth inhibition was partially but significantly rescued (Fig. 4G, H). These results suggest that YB-1 promotes BLBC cell proliferation and tumourigenesis partially by promoting KLF5 expression.

YB-1 and KLF5 co-regulate gene transcription in BLBC cells

It is noteworthy that KLF5 overexpression could not fully rescue YB-1 depletion-induced cell growth arrest (Fig. 4). We speculated that YB-1 may interact with KLF5 at the protein level. To test this

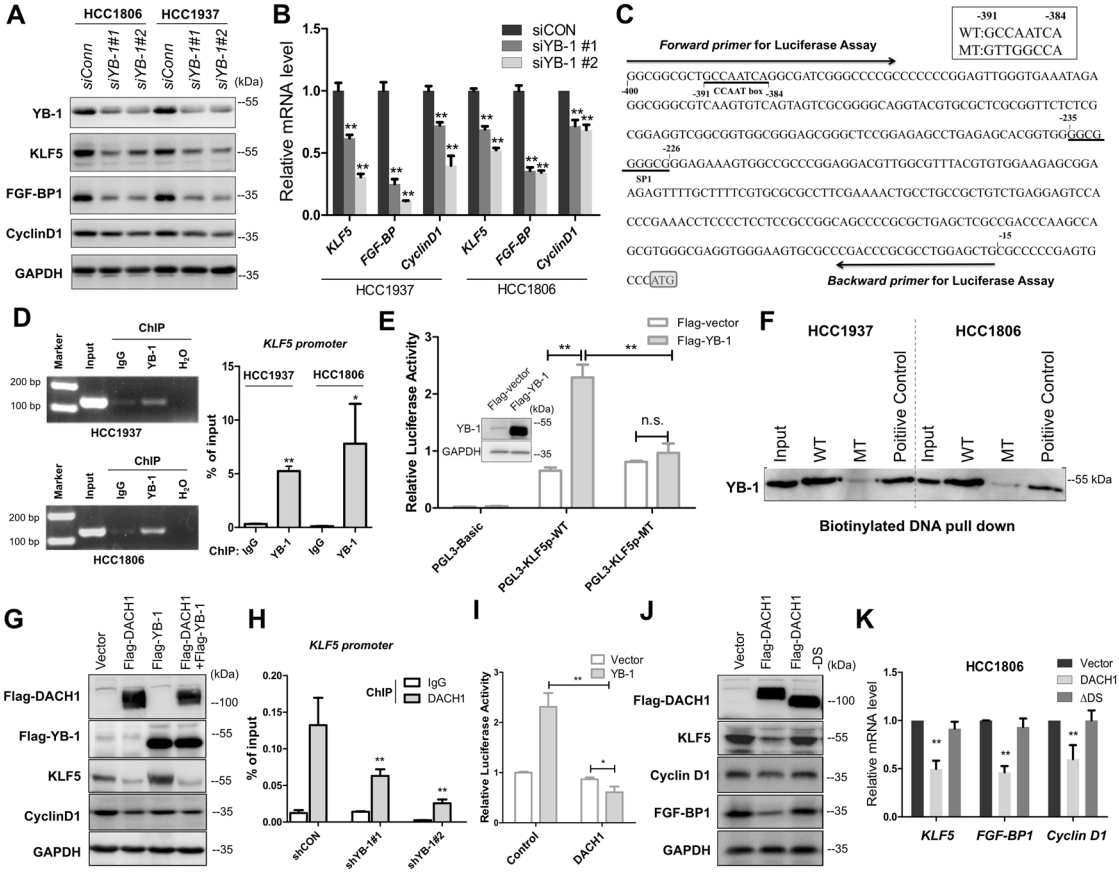

Fig. 2 YB-1 and DACH1 co-regulate KLF5 transcription. A Indicated proteins and **B** mRNA level of KLF5 and its downstream targets we detected in HCC1806 and HCC1937 cells post siRNA transfection. **C** The sequence of promoter region of *KLF5* with a potential YB-1 binding site (−391 to −384 from the start codon ATG) and primers for *Luciferase* assay were shown. **D** Chromatin immunoprecipitation (ChIP) assay performed with YB-1 antibody followed by detection of *KLF5* promoter by RT-qPCR. **E** Detection and analysis of luciferase activity in HEK293T co-transfected with YB-1 and pGL3-pKLF5 WT/Mutant promoter plasmid. **F** Proteins bound with biotin-labelled *KLF5*-promoter oligos (WT or Mutant) were pulled down by streptavidin-resin beads and then detected by YB-1 antibody. **G** Indicated protein were detected in HCC1806 cells overexpressing 3xFlag-DACH1 and/or 3xFalg-YB-1. **H** The ChIP assay was performed with DACH1 antibody in HCC1806 cells post siRNA transfection, followed by detection of *KLF5* promoter by RT-qPCR. **I** Detection and analysis of luciferase activity in HEK293T co-transfected with YB-1 and/or DACH1. **J** Indicated proteins and **K** mRNA level of KLF5 and its downstream targets we detected in HCC1806 cells of overexpressing DACH1 or its DS-deficient mutant. Data are shown as means ± SD. *P* values were calculated with two-tailed unpaired Student's *t*-test; $*P < 0.05$, $**P < 0.01$.

hypothesis, we first performed co-IP experiments and verified the interaction between YB-1 and KLF5 proteins (Fig. 5A). We further mapped their interaction in detail and demonstrated that each of the three zinc-finger domains (ZFD) in the C-terminus of KLF5 participated in the interaction (Fig. 5B, C and Supplementary Fig. S5A, B). For YB-1, the Ala/Pro-rich N-terminal (AP) domain and cold-shock domain (CSD) are responsible for its interacting with KLF5 (Fig. 5D, E).

To map the YB-1 and KLF5 co-binding landscape in the whole genome scale, we performed both Flag-YB-1 and KLF5 ChIP-sequencing in HCC1806 cells. Confluence analysis revealed that YB-1 and KLF5 contain 6,203 co-binding sites/regions (Fig. 5F), and unbiased identification of the co-binding sites showed a main GC-enriched motif (Supplementary Fig. S5C). Among these, *KLF5, CDKN1A* (coding P21, an established target of YB-1 [40] and KLF5 [41]), and known oncogenes such as *MYC*, *YY1*, *KRAS*, *and GSK3b* were included (Supplementary Fig. S5D). Most of the sites/regions (~75%) were localized in transcriptional start elements, including the promoter, 5′-UTR and 1st exon, followed by the distal intergenic region (15.33%) (Fig. 5G). Of those sites/regions, a closer spatial distance between the binding tracks (Fig. 5H) and similar distribution patterns in YB-1 and KLF5 were also observed (Fig. 5I). Moreover, KEGG/GO analysis indicated that these co-binding genes involved in cell growth and survival (Hippo signaling pathway, endocytosis, and mitophagy), cell metabolism (sphingolipid and amino acid metabolism), and transcriptional misregulation in cancer (Fig. 5J). Thus, we demonstrated that YB-1 and KLF5 interact with each other, likely in a transcriptional complex, to co-regulate a set of genes involved in breast cancer cell growth.

Keratin 16 (*KRT16*) and *lymphocyte antigen 6 family member D* (*Ly6D*) are BLBC-specific oncogenes induced by YB-1 and KLF5

To further investigate the downstream genes involved in the mechanism through which YB-1 and KLF5 collaborate to promote BLBC cell proliferation, we conducted RNA sequencing in HCC1806 and HCC1937 cells following silencing YB-1 and KLF5 expression. Among the differentially expressed genes, eleven and five genes consistently decreased or increased, respectively (Fig. 6A and Supplementary Fig. S6A). By overlapping analysis with the ChIP-sequencing data, we identified co-binding tracks of Flag-YB-1 and KLF5 on the promoters of *KRT16* and *Ly6D* (Fig. 6B). RT-qPCR further confirmed that *KRT16* and *Ly6D* were positively regulated by YB-1 and KLF5 (Fig. 6C). Upregulation of *KRT16* and *Ly6D* expression was also detected in breast cancer patients with advanced tumour grades (Supplementary Fig. S6B), like that

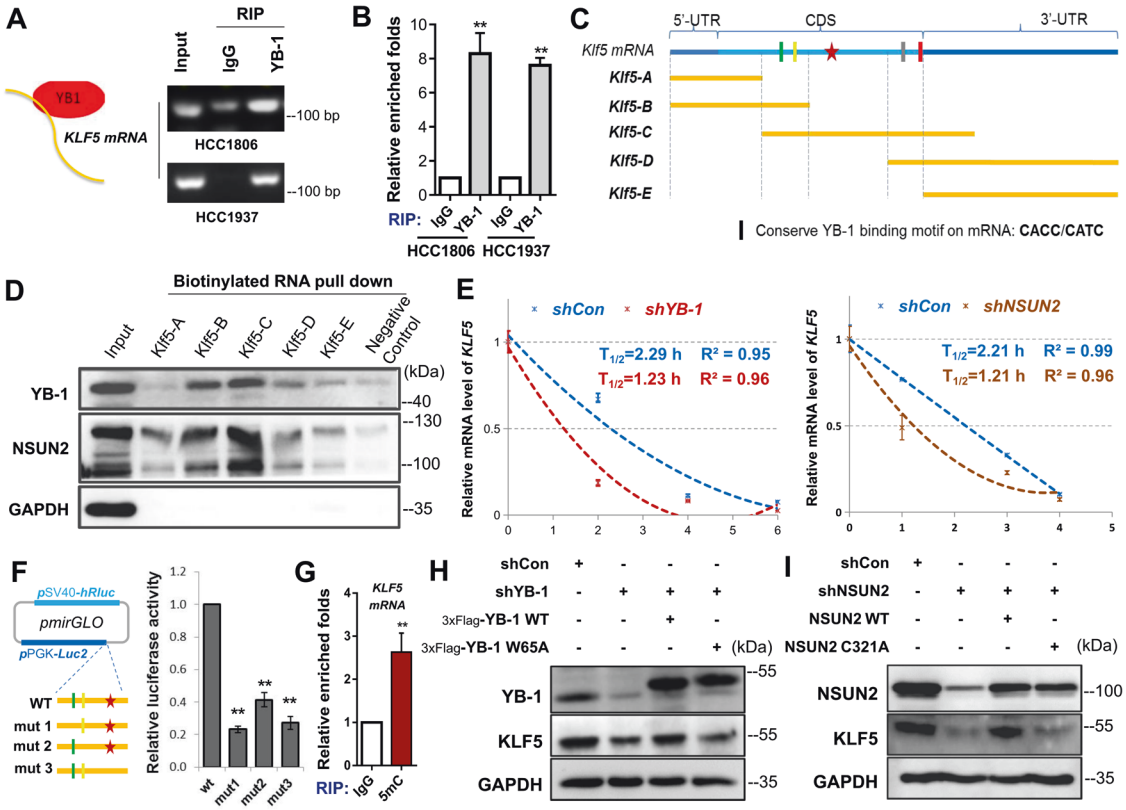

Fig. 3 YB-1 binds to and stabilizes m5C-modified *KLF5* mRNA in breast cancer cells. A, **B** RIP assay was performed to quantified the binding of YB-1 to *KLF5* mRNA in HCC1806 and HCC1937 cells. **C** The diagram of truncated *KLF5 mRNA* according to its cDNA sequence. **D** Biotin-labelled *KLF5* truncates were incubated with HCC1806 cell lysate and were pulled down by streptavidin-resin beads, and then detected by YB-1, NSUN2 and GAPDH antibodies. **E** The half-life of *KLF5* mRNA were determined in HCC1806 cells of shCon, shYB-1 and shNSUN2 by semi-qPCR, treated by 7.5 μg/mL actinomycin (ActD). **F** Relative luciferase activity of *KLF5* truncates containing three putative YB-1 binding sites in HEK293T. The indicated WT or mutated fragments were inserted into the end of *Luc2* to determine the stability of respective transcripts. **G** me-RIP and PCR detection were performed to verify the m5C modification on *KLF5* mRNA in HCC1806 cells. **H** Western blotting showing the protein expression of YB-1 and KLF5 in shYB-1 HCC1806 cells, which stably expressing 3xFlag-YB-1-WT, 3xFlag-YB-1-W65A, and vector control. **I** Western blotting showing the protein expression of NSUN2 and KLF5 in shNSUN2 HCC1806 cells, re-expressing NSUN2-WT, NSUN2-C321A, or vector control. Data are shown as means ± SD. *P* values were calculated with two-tailed unpaired Student's *t*-test; $^{*}P < 0.05$, $^{**}P < 0.01$.

of *YB-1* and *KLF5* (Fig. 1d; Supplementary Fig. S1B). Further correlation analysis of integrated mRNA data from 4712 breast cancer patients revealed significantly positive correlations among the expression of *YB-1*, *KLF5*, *KRT16*, and *Ly6D*, but a negative correlation between these four genes and *DACH1* (Fig. 6D). Based on TGCA database, we found that *KRT16* and *Ly6D* mRNA expression was specifically increased in the BLBC subtype (Fig. 6E). Consistently, the expression of *KRT16* and *Ly6D* was negatively correlated with *ESR* expression, but positively correlated with *FGF-BP1* (Supplementary Fig. S6C). Functionally, knockdown of *KRT16* and *Ly6D* suppressed BLBC cell growth (Fig. 6F), supporting the oncogenic role of the two genes in BLBCs. Clinically, high expression of either *KRT16* or *Ly6D* predicted poor overall survival (OS), recurrence-free survival (RFS), and distant metastasis-free survival (DMFS) in breast cancer patients (Fig. 6G and Supplementary Fig. S6D). These findings suggest that *KRT16* and *Ly6D* are new candidate biomarkers and therapeutic targets for BLBC.

RSK inhibition disrupts the YB-1 and KLF5 complex and suppresses BLBC growth

Phosphorylated YB-1 (pS102) is a precise indicator of aggressiveness in breast cancer patients [42, 43]. Consistently, we found that high level of YB-1 pS102 indicated poor clinical outcome in YB-1-positive breast cancer (Supplementary Fig. S7A). We then screened for the upstream kinases for YB-1 pS102 using individual pharmacological inhibitors. We found that inhibition of RSKs, rather than AKT or ERK, determines the expression of the YB-1 pS102-KLF5 axis in BLBC cells and a BLBC-patient-derived cell line (Fig. 7A and Supplementary Fig. S7B–D). We further confirmed that knockdown of RSK2, an important oncogene of the RSK family that is highly expressed in BLBCs (Supplementary Fig. S7E), decreased expression levels of YB-1 pS102, KLF5, and FGF-BP1 (Supplementary Fig. S7F). As expected, the expression of *RSK2* and *YB-1*, *KLF5*, *KRT16*, *and Ly6D* was positively correlated, while the expression of *RSK2* and *DACH1* was negatively correlated (Supplementary Fig. S7G).

We further study why pS102 was essential for YB-1-mediated induction of KLF5 expression. We used LJH685 to inhibit YB-1 pS102 and found that both YB-1-mediated transcriptional activation of *KLF5* promoter and its binding to *KLF5* promoter were suppressed (Fig. 7B–D). In addition, unlike YB-1 WT, YB-1 S102A mutant failed to activate the *KLF5* promoter (Fig. 7E) or rescue KLF5 expression (Fig. 7F). We also found that LJH685 decreased YB-1 binding to the promoters of *KRT16* and *Ly6D* (Supplementary Fig. S7H). However, treatment with the RSK inhibitors, BI-D1907 and LJH685, did not change the nuclear localization of YB-1, although YB-1 pS102 was largely inhibited (Supplementary Fig. S8A–D). Next, we suspected whether phosphorylation of YB-1 at S102 increased its interaction with KLF5. YB-1 S102A, but not WT and the S102D mutant, abrogated its interaction with KLF5 (Fig. 7G). These results suggest that phosphorylation of YB-1 at S102 is pivotal

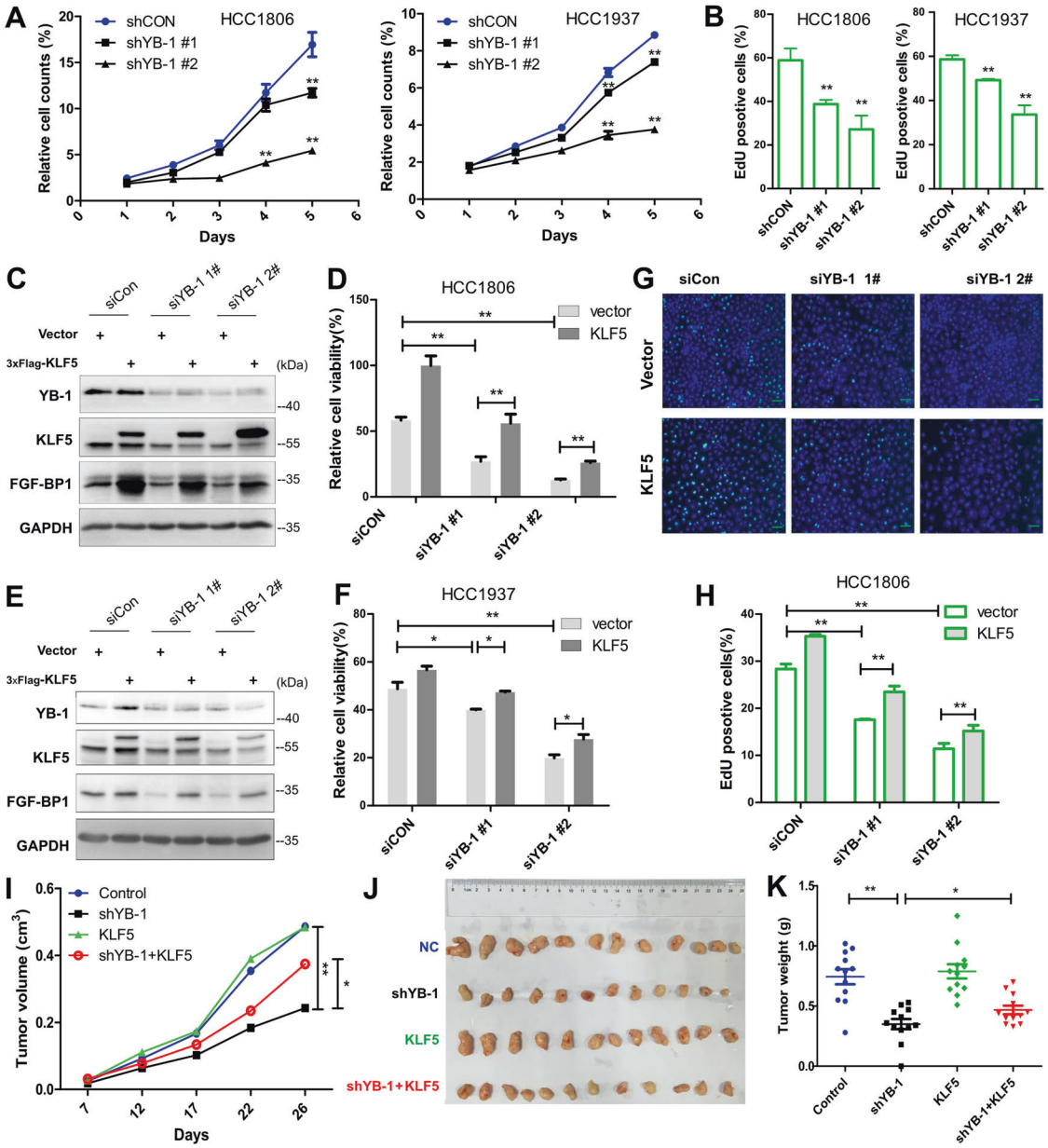

Fig. 4 YB-1 promotes BLBC cell proliferation and tumour growth partially through KLF5. A Cell viability and **B** Edu intake ratio were detected in HCC1806 and HCC1937 cells of control or YB-1 stable knockdown. **C**–**F** Western blotting showing level of indicated proteins and relative cell survival of HCC1806 cells (**C**, **D**) and HCC1937 cells (**E**, **F**) with siCon/siYB-1 transfection and 3xFlag-KLF5 overexpression, respectively. **G** Representative images and **H** statistical analysis of Edu positive HCC1806 cells post siCon/siYB-1 transfection and 3xFlag-KLF5 overexpression (scale bar=30 μm). **I**-**K** Immunodeficiency mice ($n = 6$ per group) were subcutaneously inoculated into the mammary fat pads with HCC1806 cells of shCon/shYB-1 and/or 3xFlag-KLF5 overexpression, and tumour growth was monitored every 4–5 days (**I**). All tumours were showed as (**J**) and weighted (**K**). Data are shown as means ± SD. *P* values were calculated with two-tailed unpaired Student's *t*-test; $^{*}P < 0.05$, $^{**}P < 0.01$.

for YB-1/KLF5 transcriptional complex formation and downstream target genes transcription.

Then we sought to determine whether the RSK inhibitor, LJH685, could serve as a potential therapeutic drug in BLBC. To test this, we evaluated the anti-tumour effect of LJH685 in an HCC1806 orthotopic xenograft mouse model. As expected, we observed significant suppression of tumour growth following LJH685 administration (Fig. 7H, I), although this compound showed low solubility in water and a short half-life in blood [44]. There was no marked weight loss in the LJH685-treated mice, suggesting its toxicity was acceptable (Supplementary Fig. S8E). Furthermore, we demonstrated that LJH685 decreased the expression of YB-1 pS102, KLF5, KRT16, Ly6D, and Cyclin D1, but increased cleaved-PARP1 in the xenograft tumour tissues (Supplementary Fig. S8F). Taken together, LJH685 efficiently inhibits HCC1806 cell growth in vivo and therefore represents a potential drug for the treatment of BLBC.

Finally, we examined the expression of RSK2, KRT16, Ly6D, and YB-1 pS102 in BLBC clinical tumour samples. As expected, the IHC scores of these proteins were high and correlated positively (Fig. 7J, K and Supplementary Fig. S8G), supporting the key role of the YB-1-KLF5 axis in the clinical specimens.

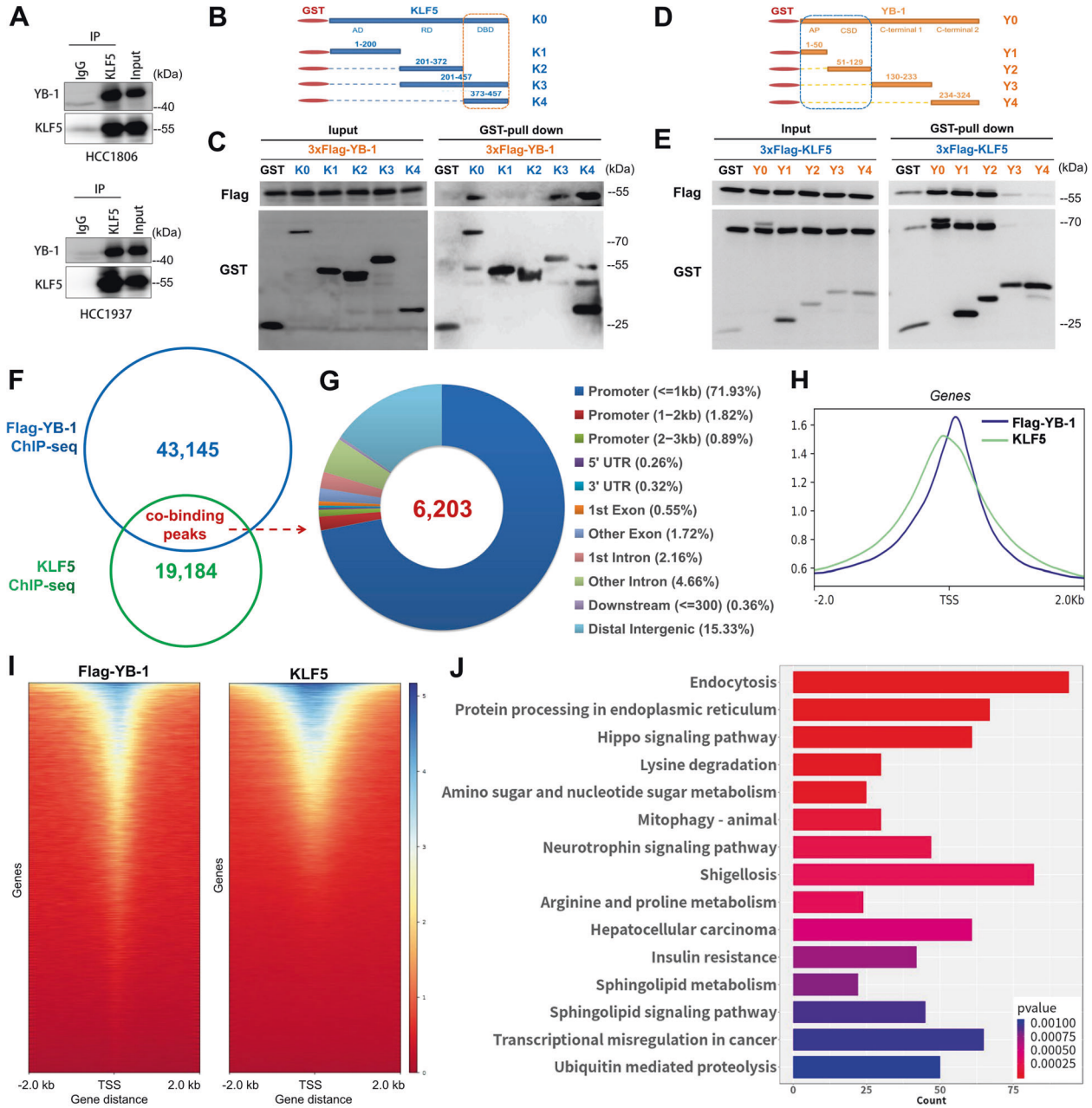

Fig. 5 YB-1 and KLF5 collaborate as co-transcriptional factors. A Co-immunoprecipitation detected the endogenous interaction between YB-1 and KLF5. **B-E** GST-pull down assay to show the binding ability of the indicated GST-labelled KLF5 truncates to 3xFlag-YB-1(**B**, **C**) or the indicated GST-labelled YB-1 truncates to 3xFlag-KLF5 (**D**, **E**), respectively. **F** Specific peaks of genomic binding were identified by Flag-YB-1 and KLF5-ChIP-sequencing in HCC1806 cells and **G** elements characteristics of overlapping regions were analyzed. **H** Peaks comparison and **I** distributing patterns of the overlapping regions suggested a co-binding model of YB-1 and KLF5. **J** KEGG/GO analysis showed YB-1 and KLF5 might co-regulate genes involving indicated pathways.

DISCUSSION

Recently, *KLF5* was identified as a candidate target gene in breast cancer risk regions, through the analyses of genome-wide interactomes by capture Hi-C array [45]. We previously reported that KLF5 was one of the major drivers of BLBC oncogenesis [3, 8, 46–50]; however, the mechanism of KLF5 specific enrichment in BLBC remains unknown. In this study, we identified the YB-1 as a master positive regulator of KLF5 specifically in BLBC (Fig. 8). Furthermore, we demonstrated that DACH1 inhibited YB-1-mediated KLF5 transcription and suppressed BLBC cell survival (Figs. 2 and 4). Given that the DACH1 promoter was highly methylated in breast cancer patients (Supplementary Fig. S8H), reactivation of DACH1 expression in BLBC with drugs, such as *Decitabine*, may be promising. Recent studies reported its RNA binding affinity is determined by NSUN2-mediated m5C modification on the CACC/CAUC motif [35, 51]; however, the biological roles of RNA-m5C have rarely been reported in cancers, including BLBC. Here, we report that YB-1 binds to and stabilizes *KLF5* mRNA through a mechanism that is likely dependent on NSUN2-mediated m5C modification of *KLF5* mRNA in BLBC cells (Fig. 3). How m5C modification of *KLF5* mRNA is regulated under physiological and pathological conditions also needs to be further explored. A recent study indicated that YB-3, a closed family member of YB-1, has a substituted function to YB-1 [52]. However,

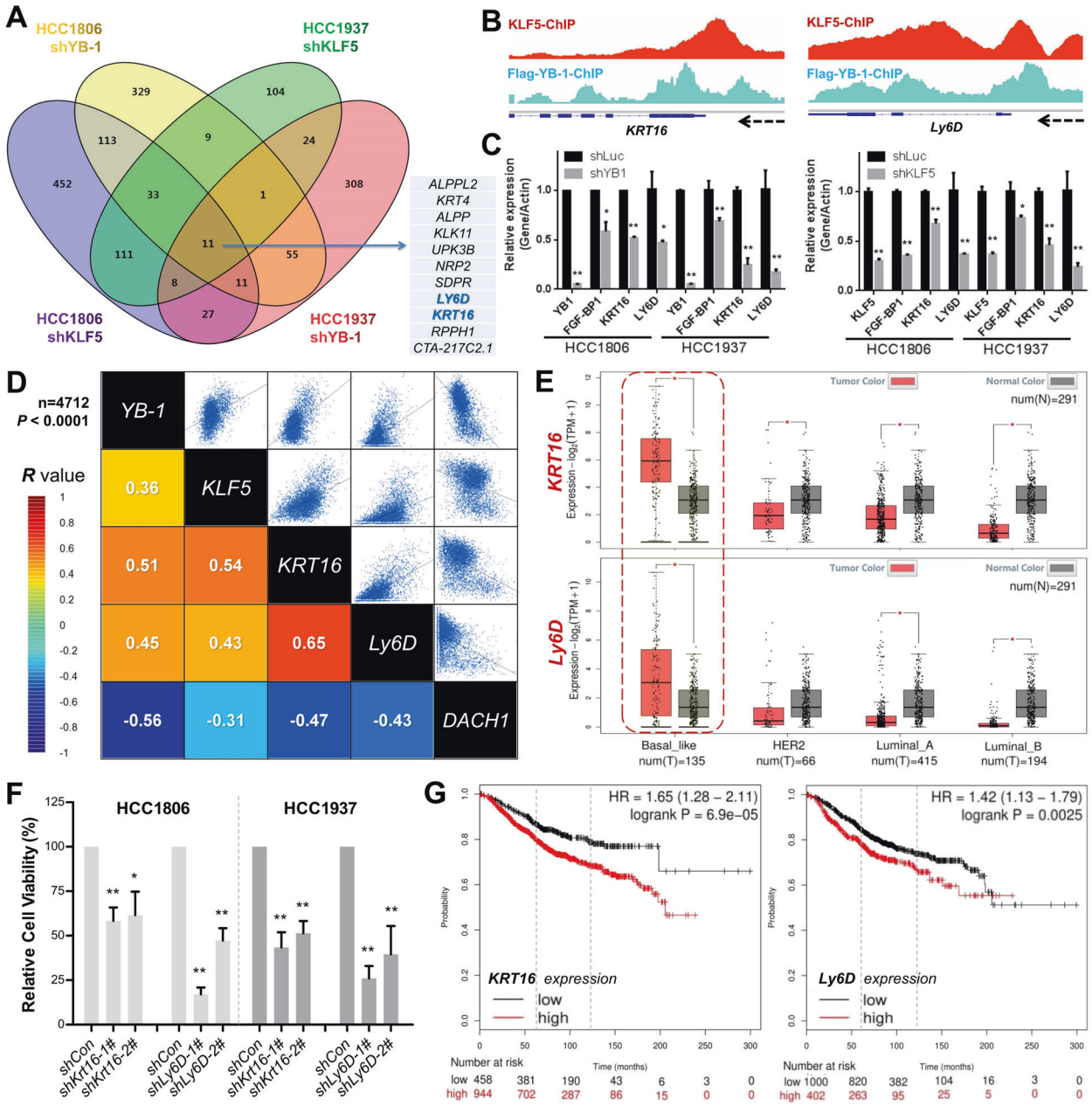

Fig. 6 ***KRT16* and *Ly6D* are BLBC-specific oncogenes controlled by YB-1 and KLF5. A** Positively regulated genes were identified by RNA-sequencing in HCC1806 and HCC1937 cells of YB-1 or KLF5 knockdown, in which 11 co-regulated genes were showed. **B** Binding tracks of Flag-YB-1 or KLF5 on the TSS region of *KRT16* or *LY6D*. **C** RT-qPCR detection of the mRNA level of *KRT16*, *LY6D*, *FGF-BP1*, and *YB-1* or *KLF5* in HCC1806 and HCC1937 cells of YB-1 or KLF5 knockdown, respectively. **D** Correlation analysis of mRNA expression among *YB-1*, *KLF5*, *KRT16*, *LY6D* and *DACH1* in 4,712 breast cancer patients (bc-GenExMiner v4.5). **E** The expression patterns of *KRT16* and *Ly6D* in breast cancers subtypes and normal tissues (GEPIA2 analysis). **F** Relative cell survival of HCC1806 and HCC1937 cells with *KRT16* or *LY6D* stable knockdown. **G** Kaplan–Meier curves showed that high expression of either *KRT16* or *Ly6D* predicted the poorer overall survival (OS) of breast cancer patients (Kaplan–Meier plotter database); 5-year and 10-year lines are indicated. Data are shown as means ± SD. *P* values were calculated with two-tailed unpaired Student's *t*-test; $^{*}P < 0.05$, $^{**}P < 0.01$.

knockdown of YB-3 did not change *KLF5* mRNA level in BLBC cells (data not shown), further suggesting the selectivity and specificity of the mechanism. Considering studies indicated ncRNAs participate in YB-1 function [53, 54], we will further characterize if any noncoding RNAs paticipating in the axis.

Interestingly, YB-1 also forms a transcriptional complex with KLF5 to regulate the transcription of several target genes (Figs. 5 and 6). Notably, Tomtom analysis of YB-1/KLF5 ChIP sites showed high enrichment of the conserved CG-rich motif of KLF5/4 (Supplementary Fig. S5C), suggesting that their functions may depend on KLF5 pre-binding. It has been speculated that YB-1 may work in an NY-1-dependent manner [55]. We propose a YB-1/KLF5 cooperative-working model in which transcription of target genes is initiated through KLF5-specific binding and formation of a transcriptional complex with YB-1; subsequently, YB-1 translocates to the nascent mRNAs. Although more evidence is required to support this promising model, our study provides a general example and the mechanism may be universal to YB-1 positive cancers (Fig. 8). In this study, we defined more than 6,000 YB-1/KLF5 co-binding regions in BLBC cells, involving hundreds of

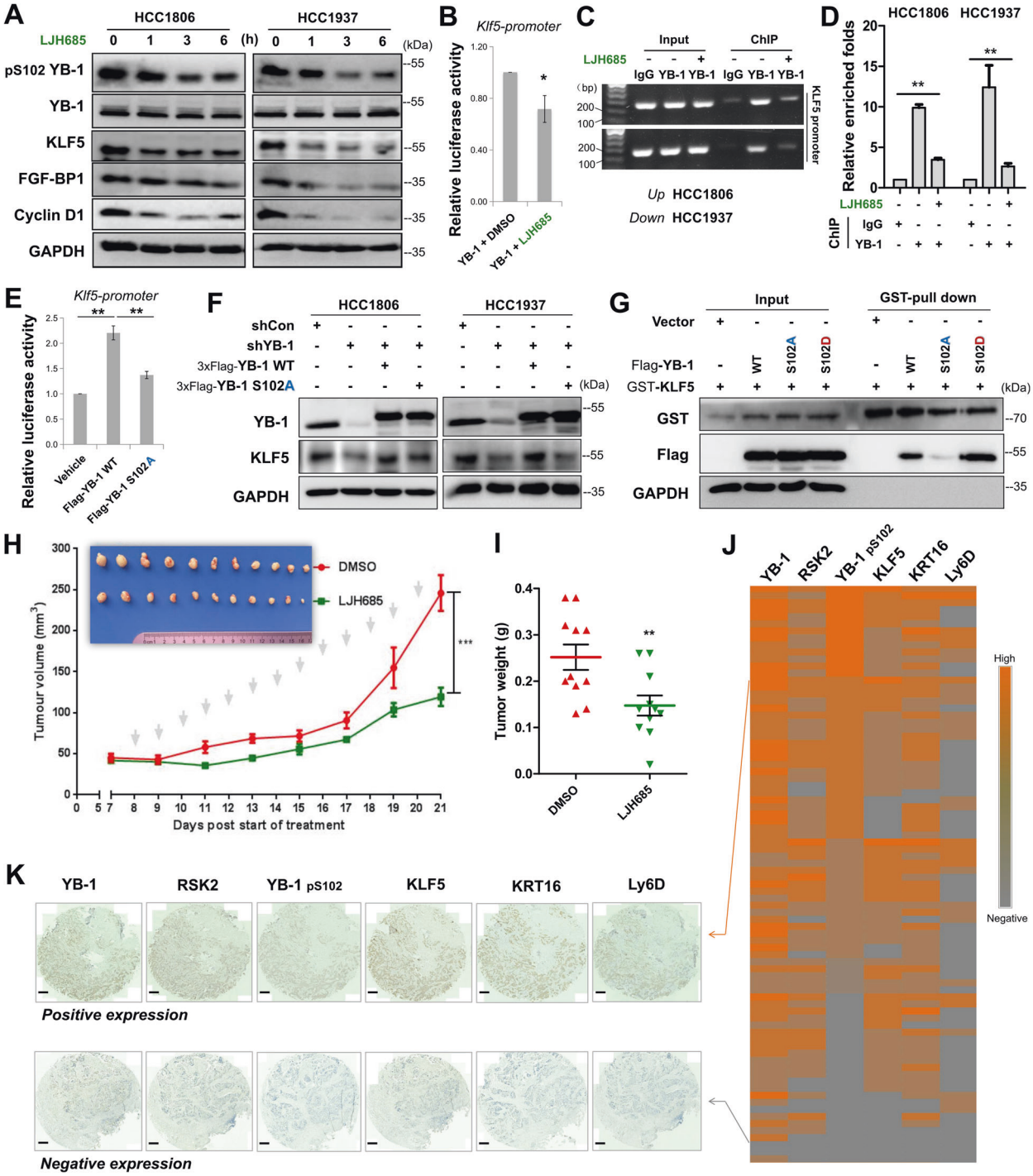

Fig. 7 RSK inhibition blocked RSK2-YB-1-KLF5 axis to suppress BLBC progression. A Western blotting showed the expression of YB-1 pSer102, YB-1, KLF5, FGF-BP1 and Cyclin D1 in HCC1806 and HCC1937 cells, post treatment with RSK inhibitor LJH685 (10 μM). GADPH was set as control. **B** Relative luciferase activity to show the transcriptional activation of *KLF5* promoter in YB-1-transfected HEK293T cells, treated with DMSO or LJH685 (10 μM). **C**, **D** ChIP was performed in HCC1806 and HCC1937 cells with the treatment of DMSO or LJH685 to detect the accessibility of YB-1 to *KLF5* promoter. **E** Relative luciferase activity of *KLF5* promoter in HEK293T cells under the expression of YB-1 WT or S102A mutant. **F** Western blotting showing the protein expression of YB-1 and KLF5 in HCC1806 and HCC1937 cells of stable YB-1 knockdown, re-expressing 3xFlag-YB-1-WT or S102A. **G** GST-pull down assay to show the affinity of GST-KLF5 to the Flag-YB-1 WT, S102A, or S102D. **H** Immunodeficiency mice ($n = 6$ per group) were subcutaneously inoculated into the mammary fat pads with HCC1806 cells, then administrated with vehicle or LJH685 (40 mg/kg), tumours' volume was minored and **I** tumours were weighted. **J** Heat map of the expressions (IHC scores) of RSK2, YB-1, pS102 YB-1, KLF5, KRT16 and LY6D in BLBC patients ($n = 82$) and **K** representative IHC images were showed (scale bar = 150 μm). Data are shown as means ± SD. *P* values were calculated with two-tailed unpaired Student's *t*-test and $P < 0.05$ is considered statistically significant.

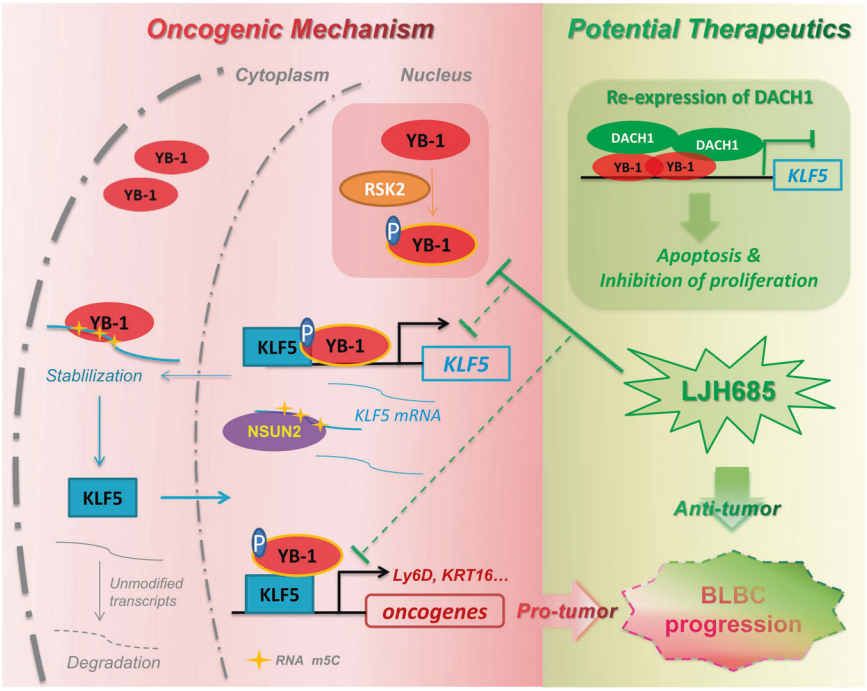

Fig. 8 Mechanism diagram for YB-1 and KLF5 promoting the BLBC progression. Oncogenes including *RSK2*, *YB-1* and *NSUN2* highly expressed in BLBC. RSK2 phosphorylates YB-1 on Ser102 and thus acitivates *KLF5* transcription; Subsequently, NSUN2 catalyzes m5C modification on *KLF5* mRNA, which can be recognized and bound by YB-1 to promote its stability. Moreover, phosphorylated YB-1 interates with KLF5 and they promote oncogenes expression, e.g. *Ly6D* and *KRT16*, which resulted in tumour cell proliferation and BLBC progression. Two strategies potentially abolish this pathway: (i) Re-expressing DACH1 can inhibit YB-1-mediated KLF5 hyper-expression and induce cell apoptosis; (ii) Inhibition of RSK2-mediated YB-1 phosphorylation by LJH685 also dramatically decreased KLF5 expression and suppressed tumour growth.

genes. We focused on *KRT16* and *Ly6D* because their functions have not been previously studied in breast cancer. KRT16 is a type I cytoskeletal protein belonging to the keratin family and is expressed in epithelial and endothelial cells [56]. Overexpression of keratins play important roles in tumourigenesis [57–60]; however, KRT16 has been poorly studied. KRT16 is overexpressed in lung adenocarcinoma and promotes lymph node metastasis via EMT [61], and is also highly expressed in BLBC cell lines, circulating tumour cells, and chemoresistant BLBCs [62, 63]. We showed that KRT16 knockdown suppressed BLBC cell growth (Fig. 6f). *Ly6D* is a marker of mammary epithelial cells and mammary carcinoma cells [64] and a potent marker for distant metastasis of ERα-positive breast cancer [65]. Increased expression of Ly6 family members indicates poor clinical outcomes in multiple cancers [66]. Here, we showed that Ly6D was specifically overexpressed in BLBCs and was important for the cancer cell growth (Fig. 6f). Based on this study, we propose a number of potential biomarkers for the diagnosis and prognosis of BLBC. Although *YB-1*, *KLF5*, *RSK2*, and *DACH1* have been previously reported as oncogenes or tumour suppressor genes in BLBC, their cooperative mechanisms were identified in this study. Additionally, *KRT16* and *Ly6D* were, for the first time, identified as highly expressed oncogenes in BLBC that indicate worse clinical outcomes (Fig. 7), and their co-expression (Supplementary Fig. S7C) further points to the potential of their clinical application in diagnosis and therapeutics, combined with the above genes.

In our study, RSKi inhibited YB-1-pS102-KLF5 more efficiently than ERKi or PI3Ki did (Supplementary Fig. S7b), suggesting RSKs mainly function in this axis in TNBC cells. RSK members have different roles in cancer [67]. We found that only RSK2 was highly expressed in BLBC patients and RSK2 depletion decreased YB-1 pS102 in BLBC cells (Supplementary Fig. S8). Thus, RSK2 is likely responsible for YB-1 activation in BLBC, although how RSK2 is deregulated in BLBC remains unclear. It was reported that irradiation, TNFα, EGF, and chemotherapy increased RSK-mediated YB-1 pS102 level, both in cytoplasm and nucleus, separately [68]. TNFα, LPS, and IL-1β have also been reported to induce KLF5 expression [69–71]. Whether the RSK2-YB-1 axis is involved in these situations requires further investigation. Phosphorylated YB-1 has been reported to promote YB-1 nuclear translocation [68, 72]. However, we found that YB-1 pS102 did not affect this process in BLBC cells (Supplementary Fig. S8). Furthermore, there is no evidence to support that YB-1 pS102 increases its binding to *KLF5* mRNA (data not shown). Instead and unexpectedly, YB-1 pS102 was required for its interaction with KLF5 and recruitment to target gene promoters (Fig. 7). This is consistent with our statement that KLF5 may serve as a crucial pioneer factor for directing the transcriptional complex to the target sites. Remarkably, CSD domain of YB-1, where the S102 site is located, is responsible for the interaction with KLF5. However, how pS102 promotes their interaction requires further study.

Two RSK inhibitors, LJH685 and ILJ308, with high efficiency and specificity have been developed [73]. However, no in vivo studies using these inhibitors have been reported yet. In this study, we observed a positive effect of LJH685 in inhibiting HCC1806-xenografts in vivo with no adverse side effects on the body weight of mice. Hence, in our opinion, it is necessary to develop RSK inhibitors for clinical application in patients with BLBC. The combination of an RSK inhibitor and other therapeutic drugs may serve as promising clinical strategies, provided the stability and solubility of RSK inhibitors would be improved in the future.

In conclusion, we demonstrated that KLF5 is a new target of YB-1 at both the transcriptional and post-transcriptional levels in BLBC cells. Moreover, YB-1 and KLF5 function as co-transcriptional factors to regulate a set of oncogenes, including *KRT16* and *Ly6D*, to promote BLBC cell proliferation. The expression of the

YB-1-KLF5 network was markedly decreased following pharmacological inhibition of RSK2. Thus, our data reveals that RSK2-YB-1-KLF5-KRT16/Ly6D is a novel oncogenic axis that regulates BLBC cell growth, and highlights novel candidates for the diagnosis and treatment of YB-1-KLF5 positive BLBCs.

METHODS

Cell culture and transfection

Basal-like breast cancer cell lines, HCC1937 and HCC1806, are purchased from American Type Culture Collection (Manassas, VA, USA) and validated via short tandem repeat analysis, and cells were cultured in Rosewell Park Memorial Institute-1640 (RPMI-1640) medium (Gibco, USA) containing 5% foetal bovine serum (FBS, Gibco). HEK293T cells were cultured in Dulbecco's modified Eagle's medium (Gibco) containing 5% FBS. All cells were maintained in an incubator with 5% CO2 at 37 °C. All plasmids and siRNA were diluted in Opti-MEM (Gibco, USA) and transfected into the tumour cell lines using Lipofectamine 2000 (Invitrogen) according to the manufacturer's recommended protocol. Plasmids were transfected into HEK293T cells using 1 μg plasmid:4 μL PEI (polyethylenimine, Plybiosciences), and cells were collected after transfection for 48 h.

Coimmunoprecipitation (co-IP) and western blotting (WB)

Cells were washed with PBS and lysed in ice-cold lysis buffer (IP lysis buffer: 150 mM NaCl, 2 mM ETDA pH 8.0, 50 mM Tris-HCl pH 7.4, 0.2% NP-40) for 30 min with a protease inhibitor (MCE, HY-K0010). Cell lysates were incubated with the indicated antibodies overnight at 4 °C, followed by incubation with protein A/G beads (Santa Cruz), Flag M2 agarose beads (Sigma), or GST-affinity beads (GE Healthcare, 17-0756-01) for 3–6 h at 4 °C. The beads were washed with cell lysis buffer three to five times. Finally, the beads were boiled in 2 × SDS buffer for 10 min at 98 °C. The samples were separated by SDS-PAGE, transferred onto polyvinylidene fluoride (PVDF) membranes, and blocked with 5% non-fat dried milk for 1 h at RT. The membranes were then incubated with the indicated primary antibody at 4 °C overnight, the corresponding HRP-conjugated secondary antibody (1:5000) for 1 h at RT, and then detected with a chemiluminescent HRP substrate (US Everbright® Inc., s6009).

Dual luciferase assays

KLF5 promoter was amplified using normal human cDNA as a template. The PCR products were cloned into the pGL3-Basic vector (Promega, USA). The constructs were confirmed by DNA sequencing. HEK293T cells were seeded in 24-well plates at 5×10^4 cells per well. After 16–24 h of culture, the cells were transfected with the KLF5 promoter reporter plasmid (0.3 μg/well) and the pRL-β-actin internal control plasmid (2.5 ng/well), together with pCMV-Flag-YB-1 plasmid (0.3 μg/well) or negative control plasmid in triplicate. At 48 h after transfection, the cells were collected

Chromatin immunoprecipitation (ChIP) and sequencing

ChIP assay was performed using the HCC1937 and HCC1806 cell lines following the manufacturer's instructions (Abcam, Cambridge, MA, USA). Protein A/G beads were first mixed with an equal amount of anti-YB-1 antibody or rabbit IgG (Proteintech) and incubated overnight at 4 °C. HCC1937 and HCC1806 cells were fixed with 3.7% formaldehyde. Ten minutes later, glycine (125 mM) was added to quench the formaldehyde and terminate the cross-linking reaction. Cells were scraped into an Eppendorf (EP) tube and centrifuged at 1000 × g at 4 °C for 10 min. The supernatant was aspirated off and the pellet was resuspended in cytoplasmic lysis buffer (5 mM PIPES pH 8.0, 85 mM KCl, 0.5% Nonidet P-40 with protease inhibitors; 1000 μL per 1×10^7 cells). The cell suspension was centrifuged at 4000 × g for 5 min at 4 °C. Finally, the pellet was resuspended in nuclear lysis buffer (50 mM Tris-HCl pH 8.1,10 mM EDTA, 1% SDS with protease inhibitors; 500 μL per 1×10^7 cells) and then sonicated for ten cycles, with 30 s on and 30 s off for each cycle. The next day, the DNA-protein complex was mixed with the antibody-A/G beads complex and incubated at 4 °C for 10 h. The chromosomal DNA was purified and analyzed by quantitative PCR or sent for high-throughput sequencing (Igenebook, Wuhan). The data were analyzed by LC Biotech.

Oligo pull-down assays

HCC1937 and HCC1806 cells growing in a 100-mm dish were collected in 1 mL of cell lysis buffer at 4 °C. The cell lysates were centrifuged at 12,000 × g for 15 min. The supernatant was pre-incubated with 25 μL streptavidin-resin beads (Thermo Fisher Scientific, Waltham, MA, USA) for at least 1 h at 4 °C. Poly(dI-dC) (10 μg, Thermo Fisher Scientific) was incubated with 1 mL of 3× diluted precleared HCC1937 and HCC1806 cell lysates in the presence of 0.5 μg biotinylated double-stranded oligonucleotides at 4 °C overnight. The next day, another 25 μL volume of streptavidin beads was added and incubated for at least 1 h at 4 °C. Streptavidin beads were collected by centrifugation at 5000 × g and washed with lysis buffer four times. The bound proteins were collected by adding 30 μL of 2×SDS buffer. YB-1 protein was detected by WB assay.

Immunohistochemical staining

Paraffin-embedded clinical BLBC specimens were obtained from The First Affiliated Hospital, Zhengzhou University, Zhengzhou, China. Human and mouse tumour specimen slides were incubated at 60 °C for 2 h and subjected to conventional IHC. The BLBC specimens' IHC was approved by Ethics Committee of Henan Provincial People's Hospital (#2020–205).

Quantitative reverse transcription PCR and RNA sequencing

TRIzol reagent (15596–026, Invitrogen) was used to extract total RNA. HiScript® II QRT SuperMix (Vazyme, R223-01) was used to perform reverse transcription. Quantitative PCR was performed using the SYBR™ Green Select Master Mix system (Invitrogen, 4472908). RNA sequencing was performed and analyzed by Igenebook (Wuhan, China).

RNA immunoprecipitation (RIP), RNA biotinylation, and RNA pull-down assays

The RIP assay was performed according to the manufacturer's manual of the Magna RIP Kit (Catalog No. 17–700, Millipore). Cell lysates were supplemented with RiboLock RNAase inhibitor (0.2 U/μL, Thermo, EO0384). Truncated KLF5 templates were in vitro transcribed using TranscriptAid™ T7 High Yield Transcription Kit (Thermo, K0441) and the generated RNAs were purified by chloroform extraction and isopropanol precipitation. The purified RNAs were biotinylated using the Pierce™ RNA 3′-End Desthiobiotinylation Kit (Thermo Fisher Scientific, 20163). RNA pull-down assay was performed according to the protocol described previously [13]. using the Pierce™ Magnetic RNA-Protein Pull-Down Kit (Thermo Fisher Scientific, 20164) reagents.

Tumourigenesis in nude mice

HCC1806 cells with stable YB-1 knockdown and/or KLF5 overexpression were prepared by lentiviral infection and selected using blasticidin and puromycin, respectively. Knockdown of YB-1 and overexpression of KLF5 were confirmed by WB. Twenty-four female nude mice (6-week-old) were randomly distributed into four groups (NC, shYB-1, KLF5, and shYB-1 + KLF5; each group contained six mice). HCC1806 cells (1×10^6) were injected subcutaneously into the mammary fat pads of the mice. The length and width of the tumour were measured every five days using a Vernier calipers. The tumour volumes were calculated as follows: tumour volume (mm^3) = $0.5 \times \text{length} \times \text{width}^2$. The mice were sacrificed on day 26, and the tumours were harvested and weighed. The animal experiment was approved (SMKX-20160305-08) by the Animal Ethics Committee of the Kunming Institute of Zoology, CAS.

Administration of LJH685 in tumour burden mice

HCC1806 cells (6×10^5) were injected subcutaneously into both the left and right mammary fat pads of twelve female nude mice (6–7-week-old). After seven days, the tumour volume and weight of mice were measured, and mice were randomly distributed into two groups. The mice were then treated with LJH685 (MCE, HY-19712) or NC by intraperitoneal injection daily. The tumour volume and mouse weight were measured every other day. The mice were sacrificed on day 21, and the tumours were harvested and weighed. LJH685 was prepared by adding each of the following solvents in sequential order; 10% DMSO, 40% PEG300, 5% Tween-80, and 45% saline. The drug solution was freshly prepared to avoid freeze thawing that could cause drug precipitation.

Statistical analysis

Student's *t* test (2-tailed) was used to compare differences between two groups. One-way ANOVA comparison test was used to analyze the differences among multiple groups. Data are presented as means ± standard deviation (SD). *P* values of <0.05 were considered significant. All

statistical data were calculated using the GraphPad Prism 8 (GraphPad Software Inc., La Jolla, CA, USA).

DATA AVAILABILITY

High throughput sequencing data are available at https://doi.org/10.6084/m9.figshare.13605839.v1 and https://doi.org/10.6084/m9.figshare.13605833.v1. Original IHC images are available at https://doi.org/10.6084/m9.figshare.16621180.v1. Other datasets and materials are available from the corresponding author upon reasonable request.

REFERENCES

1. Holm K, Hegardt C, Staaf J, Vallon-Christersson J, Jönsson G, Olsson H, et al. Molecular subtypes of breast cancer are associated with characteristic DNA methylation patterns. Breast Cancer Res. 2010;12:R36.
2. Lehmann BD, Bauer JA, Chen X, Sanders ME, Chakravarthy AB, Shyr Y, et al. Identification of human triple-negative breast cancer subtypes and preclinical models for selection of targeted therapies. J Clin Invest. 2011;121:2750–67.
3. Liu R, Shi P, Zhou Z, Zhang H, Li W, Zhang H, et al. Krüpple-like factor 5 is essential for mammary gland development and tumourigenesis. J Pathol. 2018;246:497–507.
4. Luo Y, Chen C. The roles and regulation of the KLF5 transcription factor in cancers. Cancer Sci. 2021;112:2097–117.
5. Wang C, Nie Z, Zhou Z, Zhang H, Liu R, Wu J, et al. The interplay between TEAD4 and KLF5 promotes breast cancer partially through inhibiting the transcription of p27(Kip1). Oncotarget. 2015;6:17685–97.
6. Zheng HQ, Zhou Z, Huang J, Chaudhury L, Dong JT, Chen C. Kruppel-like factor 5 promotes breast cell proliferation partially through upregulating the transcription of broblast growth factor binding protein 1. Oncogene. 2009;28:3702–13.
7. Xia H, Wang C, Chen W, Zhang H, Chaudhury L, Zhou Z, et al. Krüppel-like factor 5 transcription factor promotes microsomal prostaglandin E2 synthase 1 gene transcription in breast cancer. J Biol Chem. 2013;288:26731–40.
8. Jia L, Zhou Z, Liang H, Wu J, Shi P, Li F, et al. KLF5 promotes breast cancer proliferation, migration and invasion in part by upregulating the transcription of TNFAIP2. Oncogene. 2016;35:2040–51.
9. Tong D, Czerwenka K, Heinze G, Ryffel M, Schuster E, Witt A, et al. Expression of KLF5 is a prognostic factor for disease-free survival and overall survival in patients with breast cancer. Clin Cancer Res. 2006;12:2442–8.
10. Liu R, Zhou Z, Zhao D, Chen C. The induction of KLF5 transcription factor by progesterone contributes to progesterone-induced breast cancer cell proliferation and dedifferentiation. Mol Endocrinol. 2011;25:1137–44.
11. Li Z, Dong J, Zou T, Du C, Li S, Chen C, et al. Dexamethasone induces docetaxel and cisplatin resistance-partially through up-regulating Kruppel-like factor 5 in triple-negative breast cancer. Oncotarget. 2017;8:11555–65.
12. Chen CH, Yang N, Zhang Y, Ding J, Zhang W, Liu R, et al. Inhibition of super enhancer downregulates the expression of KLF5 in basal-like breast cancers. Int J Biol Sci. 2019;15:1733–42.
13. Stratford AL, Habibi G, Astanehe A, Jiang H, Hu K, Park E, et al. Epidermal growth factor receptor (EGFR) is transcriptionally induced by the Y-box binding protein-1 (YB-1) and can be inhibited with Iressa in basal-like breast cancer, providing a potential target for therapy. Breast Cancer Res. 2007;9:R61.
14. Goodarzi H, Liu X, Nguyen HC, Zhang S, Fish L, Tavazoie SF. Endogenous tRNA-derived fragments suppress breast cancer progression via YBX1 displacement. Cell. 2015;161:790–802.
15. Basaki Y, Taguchi K, Izumi H, Murakami Y, Kubo T, Hosoi F, et al. Y-box binding protein-1 (YB-1) promotes cell cycle progression through CDC6-dependent pathway in human cancer cells. Eur J Cancer. 2020;46:954–65.
16. El-Naggar AM, Veinotte CJ, Cheng H, Grunewald TG, Negri GL, Somasekharan SP, et al. Translational activation of HIF1 alpha by YB-1 promotes sarcoma metastasis. Cancer Cell. 2015;27:682–97.
17. Kohno Y, Matsuki Y, Tanimoto A, Izumi H, Uchiumi T, Kohno K, et al. Expression of Y-box-binding protein dbpC/contrin, a potentially new cancer/testis antigen. Br J Cancer. 2006;94:710–6.
18. Harada M, Kotake Y, Ohhata T, Kitagawa K, Niida H, Matsuura S, et al. YB-1 promotes transcription of cyclin D1 in human non-small-cell lung cancers. Genes Cells. 2014;19:504–16.
19. To K, Fotovati A, Reipas KM, Law JH, Hu K, Wang J, et al. Y-box binding protein-1 induces the expression of CD44 and CD49f leading to enhanced self-renewal, mammosphere growth, and drug resistance. Cancer Res. 2010;70:2840–51.
20. Guo T, Kong J, Liu Y, Li Z, Xia J, Zhang Y, et al. Transcriptional activation of NANOG by YBX1 promotes lung cancer stem-like properties and metastasis. Biochem Bioph Res Co. 2017;487:153–9.
21. Jurchott K, Bergmann S, Stein U, Walther W, Janz M, Manni I, et al. YB-1 as a cell cycle-regulated transcription factor facilitating cyclin A and cyclin B1 gene expression. J Biol Chem. 2003;278:27988–96.
22. Basaki Y, Hosoi F, Oda Y, Fotovati A, Maruyama Y, Oie S, et al. Akt-dependent nuclear localization of Y-box-binding protein 1 in acquisition of malignant characteristics by human ovarian cancer cells. Oncogene. 2007;26:2736–46.
23. Donaubauer EM, Hunzicker-Dunn ME. Extracellular signal-regulated Kinase (ERK)-dependent phosphorylation of Y-box-binding protein 1 (YB-1) enhances gene expression in granulosa cells in response to follicle-stimulating hormone (FSH). J Biol Chem. 2016;291:12145–60.
24. Stratford AL, Fry CJ, Desilets C, Davies AH, Cho YY, Li Y, et al. Y-box binding protein-1 serine 102 is a downstream target of p90 ribosomal S6 kinase in basal-like breast cancer cells. Breast Cancer Res. 2008;10:R99.
25. Habibi G, Leung S, Law JH, Gelmon K, Masoudi H, Turbin D, et al. Redefining prognostic factors for breast cancer: YB-1 is a stronger predictor of relapse and disease-specific survival than estrogen receptor or HER-2 across all tumour subtypes. Breast Cancer Res. 2008;10:R86.
26. Huang J, Tan PH, Li KB, Matsumoto K, Tsujimoto M, Bay BH. Y-box binding protein, YB-1, as a marker of tumour aggressiveness and response to a adjuvant chemotherapy in breast cancer. Int J Oncol. 2005;26:607–13.
27. Wu K, Chen K, Wang C, Jiao X, Wang L, Zhou J, et al. Cell fatefactor DACH1 represses YB-1-mediated oncogenic transcription and translation. Cancer Res. 2014;74:829–39.
28. Wu K, Yang Y, Wang C, Davoli MA, D'Amico M, Li A, et al. DACH1 inhibits transforming growth factor-beta signaling through binding Smad4. J Biol Chem. 2003;278:51673–84.
29. Popov VM, Zhou J, Shirley LA, Quong J, Yeow WS, Wright JA, et al. The cell fate determination factor DACH1 is expressed in estrogen receptor-alpha-positive breast cancer and represses estrogen receptor-alpha signaling. Cancer Res. 2009; 69:5752–60.
30. Wu K, Liu M, Li A, Donninger H, Rao M, Jiao X, et al. Cell fate determination factor DACH1 inhibits c-Jun-induced contact-independent growth. Mol Biol Cell. 2007;18:755–67.
31. Kozmik Z, Pfeffer P, Kralova J, Paces J, Paces V, Kalousova A, et al. Molecular cloning and expression of the human and mouse homologues of the Drosophila dachshund gene. Dev Genes Evol. 1999;209:537.
32. Powe DG, Dhondalay GK, Lemetre C, Allen T, Habashy HO, Ellis IO, et al. DACH1: its role as a classifier of long term good prognosis in luminal breast cancer. PLoS One. 2014;9:e84428.
33. Wu K, Chen K, Wang C, Jiao X, Wang L, Zhou J, et al. Cell fate factor DACH1 represses YB-I-mediated oncogenic transcription and translation. Cancer Res. 2014;73:829–39.
34. Zhang E, He X, Zhang C, Su J, Lu X, Si X, et al. A novel long noncoding RNA HOXC-AS3 mediates tumourigenesis of gastric cancer by binding to YBX1. Genome Biol. 2018;19:1–15.
35. Chen X, Li A, Sun BF, Yang Y, Han YN, Yuan X, et al. 5-methylcytosine promotes pathogenesis of bladder cancer through stabilizing mRNAs. Nat Cell Biol 2019; 21:978–90.
36. Yang Y, Wang L, Han X, Yang WL, Zhang M, Ma HL, et al. RNA 5-methylcytosine facilitates the maternal-to-zygotic transition by preventing maternal mRNA decay. Mol Cell. 2019;75:1188–202.e11.
37. Zou F, Tu R, Duan B, Yang Z, Ping Z, Song X, et al. Drosophila YBX1 homolog YPS promotes ovarian germ line stem cell development by preferentially recognizing 5-methylcytosine RNAs. Proc Natl Acad Sci USA. 2020;117:3603–9.
38. Trixl L, Lusser A. The dynamic RNA modification 5-methylcytosine and its emerging role as an epitranscriptomic mark. Wiley Interdiscip Rev RNA. 2019; 10:1–17.
39. Wei WJ, Mu SR, Heiner M, Fu X, Cao LJ, Gong XF, et al. YB-1 binds to CAUC motifs and stimulates exon inclusion by enhancing the recruitment of U2AF to weak polypyrimidine tracts. Nucleic Acids Res. 2012;40:8622–36.
40. Su W, Feng S, Chen X, Yang X, Mao R, Guo C, et al. Silencing of long noncoding RNA MIR22HG triggers cell survival/death signaling via oncogenes YBX1, MET, and p21 in lung cancer. Cancer Res. 2018;78:3207–19.
41. Chen Z, Wu Q, Ding Y, Zhou W, Liu R, Chen H, et al. YD277 suppresses triple-negative breast cancer partially through activating the endoplasmic reticulum stress pathway. Theranostics 2017;7:2339–49.
42. Stratford AL, Reipas K, Hu K, Fotovati A, Brough R, Frankum J, et al. Targeting p90 ribosomal S6 kinase eliminates tumour-initiating cells by inactivating Y-box binding protein-1 in triple-negative breast cancers. Stem Cells. 2012; 30:1338–48.
43. Shibata T, Watari K, Kawahara A, Sudo T, Hattori S, Murakami Y, et al. Targeting phosphorylation of Y-box–binding protein YBX1 by TAS0612 and everolimus in overcoming antiestrogen resistance. Mol Cancer Ther. 2020;19:882–94.
44. Casalvieri KA, Matheson CJ, Backos DS, Reigan P. Selective Targeting of RSK Isoforms in Cancer. Trends Cancer. 2017;3:302–12.
45. Beesley J, Sivakumaran H, Moradi-Marjaneh M, Lima LG, Hillman KM, Kaufmann S, et al. Chromatin interactome mapping at 139 independent breast cancer risk signals. Genome Biol. 2020;21:1–19.

46. Qin J, Zhou Z, Chen W, Wang C, Zhang H, Ge G, et al. BAP1 promotes breast cancer cell proliferation and metastasis by deubiquitinating KLF5. Nat Commun. 2015;6:1–12.
47. Wu Y, Qin J, Li F, Yang C, Li Z, Zhou Z, et al. USP3 promotes breast cancer cell proliferation by deubiquitinating KLF5. J Biol Chem 2019;294:17837–47.
48. Liu R, Shi P, Nie Z, Liang H, Zhou Z, Chen W, et al. Mifepristone suppresses basal triple-negative breast cancer stem cells by down-regulating KLF5 expression. Theranostics 2016;6:533–44.
49. Shi P, Liu W, Tala, Wang H, Li F, Zhang H, et al. Metformin suppresses triple-negative breast cancer stem cells by targeting KLF5 for degradation. Cell Disco. 2017;3:17010.
50. Chen C, Zhou Y, Zhou Z, Sun X, Otto KB, Uht RM, et al. Regulation of KLF5 involves the Sp1 transcription factor in human epithelial cells. Gene. 2004;330:133–42.
51. Yang XJ, Zhu H, Mu SR, Wei WJ, Yuan X, Wang M, et al. Crystal structure of a Y-box binding protein 1 (YB-1)–RNA complex reveals key features and residues interacting with RNA. J Biol Chem. 2019;294:10998–1010.
52. Lyabin DN, Eliseeva IA, Smolin EA, Doronin AN, Budkina KS. Kulakovskiy IV, et al. YB-3 substitutes YB-1 in global mRNA binding. RNA Biol. 2020;17:487–99.
53. Tang L, Wei D, Xu X, Mao X, Mo D, Yan L, et al. Long non-coding RNA MIR200CHG promotes breast cancer proliferation, invasion, and drug resistance by interacting with and stabilizing YB-1. NPJ Breast Cancer. 2021;7:94.
54. Wang M, Dai M, Wang D, Tang T, Xiong F, Xiang B, et al. The long noncoding RNA AATBC promotes breast cancer migration and invasion by interacting with YBX1 and activating the YAP1/Hippo signaling pathway. Cancer Lett. 2021;512:60–72.
55. Dolfini D, Mantovani R. Targeting the Y/CCAAT box in cancer: YB-1 (YBX1) or NF-Y. Cell Death Differ. 2013;20:676–85.
56. Steen K, Chen D, Wang F, Majumdar R, Chen S, Kumar S, et al. A role for keratins in supporting mitochondrial organization and function in skin keratinocytes. Mol Biol Cell. 2020;31:1103–11.
57. Saha SK, Kim K, Yang GM, Cho HY, Cho SG. Cytokeratin 19 (KRT19) has a role in the reprogramming of cancer stem cell-like cells to less aggressive and more drug-sensitive cells. Int J Mol Sci. 2018;19:1423.
58. Ricciardelli C, Lokman NA, Pyragius CE, Ween MP, Macpherson AM, Ruszkiewicz A, et al. Keratin 5 overexpression is associated with serous ovarian cancer recurrence and chemotherapy resistance. Oncotarget. 2017;8:17819–32.
59. Wu H, Wang K, Liu W, Hao Q. Recombinant adenovirus-mediated overexpression of PTEN and KRT10 improves cisplatin resistance of ovarian cancer in vitro and in vivo. Genet Mol Res. 2015;14:6591–7.
60. Mockler D, Escobar-Hoyos LF, Akalin A, Romeiser J, Shroyer AL, Shroyer KR. Keratin 17 Is a Prognostic Biomarker in Endocervical Glandular Neoplasia. Am J Clin Pathol. 2017;148:264–73.
61. Yuanhua L, Pudong Q, Wei Z, Yuan W, Delin L, Yan Z, et al. TFAP2A induced KRT16 as an oncogene in lung adenocarcinoma via EMT. Int J Biol Sci. 2019;15:1419–28.
62. Joosse SA, Hannemann J, Spötter J, Bauche A, Andreas A, Müller V, et al. Changes in keratin expression during metastatic progression of breast cancer: impact on the detection of circulating tumour cells. Clin Cancer Res. 2012;18:993–1003.
63. Yu KD, Zhu R, Zhan M, Rodriguez AA, Yang W, Wong S, et al. Identification of prognosis-relevant subgroups in patients with chemoresistant triple-negative breast cancer. Clin Cancer Res 2013;19:2723–33.
64. Tsukada Y, Sasaki T, Hanyu K, Enami J. Expression of ly6d on the surface of normal and neoplastic mammary epithelial cells of the mouse. Jpn J Cancer Res. 2005;93:986–93.
65. Mayama A, Takagi K, Suzuki H, Sato A, Onodera Y, Miki Y, et al. OLFM4, LY6D and S100A7 as potent markers for distant metastasis in estrogen receptor-positive breast carcinoma. Cancer Sci. 2018;109:3350–9.
66. Upadhyay G. Emerging role of novel biomarkers of Ly6 gene family in pan cancer. Adv Exp Med Biol. 2019;1164:47–61.
67. Houles T, Roux PP. Defining the role of the RSK isoforms in cancer. Semin Cancer Biol. 2018;48:53–61.
68. Tiwari A, Rebholz S, Maier E, Dehghan-Harati M, Zips D, Sers C, et al. Stress-induced phosphorylation of nuclear YB-1 depends on nuclear trafficking of p90 ribosomal S6 kinase. Int J Mol Sci. 2018;19:2441.
69. Ma D, Chang LY, Zhao S, Zhao JJ, Xiong YJ, Cao FY, et al. KLF5 promotes cervical cancer proliferation, migration and invasion in a manner partly dependent on TNFRSF11a expression. Sci Rep. 2017;7:15683.
70. Chanchevalap S, Nandan MO, McConnell BB, Charrier L, Merlin D, Katz JP, et al. Kruppel-like factor 5 is an important mediator for lipopolysaccharide- induced proinflammatory response in intestinal epithelial cells. Nucleic Acids Res. 2006;34:1216–23.
71. Mori A, Moser C, Lang SA, Hackl C, Gottfried E, Kreutz M, et al. Up-regulation of Krüppel-like factor 5 in pancreatic cancer is promoted by interleukin-1beta signaling and hypoxia-inducible factor-1alpha. Mol Cancer Res. 2009;7:1390–8.
72. Jayavelu AK, Schnöder TM, Perner F, Herzog C, Meiler A, Krishnamoorthy G, et al. Splicing factor YBX1 mediates persistence of JAK2-mutated neoplasms. Nature. 2020;588:157–63.
73. Casalvieri KA, Matheson CJ, Backos DS, Reigan P. Selective targeting of RSK isoforms in cancer. Trends Cancer. 2017;3:302–12.

ACKNOWLEDGEMENTS

We thank Prof. Yun-Gui Yang (Beijing Institute of Genomics, Chinese Academy of Sciences) for kindly offering pCMV-NSUN2 wt/c321a constructs.

AUTHOR CONTRIBUTIONS

CC, MZ, XM and DJ designed and supervised the study. DJ, TQ, JP, and SL performed most of the experiments and analyses. WR, JS, CHC, YW and Tala participated in some experiments. CY and YW performed and analyzed clinical and experimental IHC data. WL, RL, JZ and KW participated in discussion. DJ, CC, and TQ draft the manuscript. All authors discussed and finalized this paper.

FUNDING

This work was supported by National Key R&D Program of China (2020YFA0112300 and 2020YFA0803200), National Science Foundation of China (81672639 to ZZ; 81830087, U2102203 and 31771516 to CC; 81802671, 81872414 and 82173014 to DJ; 81972791 to XM), CAS "Light of West China" Young Scholar Program to DJ, Yunnan Fundamental Research Projects (202001AW070018, 202101AS070050, and 2019FB112), and Project of Innovative Research Team of Yunnan Province (2019HC005)

COMPETING INTERESTS

The authors declare no competing interests.

ETHICS APPROVAL

Approvals of animal and human samples-related experiments were described in Methods.

ADDITIONAL INFORMATION

Supplementary information The online version contains supplementary material available at https://doi.org/10.1038/s41418-021-00920-x.

Correspondence and requests for materials should be addressed to Xiaoyun Mao, Zhongmei Zhou or Ceshi Chen.